

Development and Research of a Laser Photo-Acoustic SF₆ Gas Analyzer¹

I. V. Sherstov*, V. A. Vasiliev, K. G. Zenov, R. V. Pustovalova,
V. V. Spitsin, and S. B. Chernikov

*Institute of Laser Physics Siberian Branch, Russian Academy of Sciences,
Novosibirsk, 630090 Russia*

**e-mail: sherstov@ngs.ru*

Received February 26, 2016; in final form, December 5, 2016

Abstract—An analysis of various optical schemes for the development of a laser SF₆ gas analyzer based on a CO₂ laser operating in free-running mode and a resonant photo-acoustic detector (PAD) is presented. The use of a sealed gas-filled cell to normalize PAD signals on the absorbed power in the cell is suggested. Compensation for the influence of the tuning of the CO₂ laser wavelength near 10.6 μm on measured SF₆ concentration is possible. The results of experimental studies of a laser photo-acoustic SF₆ gas analyzer at various concentrations, including in the air flow, are presented. It is shown experimentally that the relative measurement error of the SF₆ concentration due to the instability of the laser radiation wavelength does not exceed 5% in the range from ~80 ppb to 40 ppm. The limit of the sensitivity of the developed gas analyzer was ~1 ppb SF₆.

DOI: 10.1134/S0020441217030253

1. INTRODUCTION

Sulphur hexafluoride (SF₆; elegas) is widely used in the power industry and communication channels as an effective insulator gas. Modern high-voltage equipment, operating at a voltage greater than 110 kV is usually mounted inside dielectric covers that are filled with pure SF₆ to an operating pressure of ~5 atm. A number of devices have been designed to control leaks of SF₆ from various gas-filled units and vessels under pressure. Commercially available SF₆ gas analyzers have a limit sensitivity ~0.1–1 ppm. Development of new gas detectors with higher sensitivity to sulfur hexafluoride is relevant.

Among gas analyzers that are designed to detect various impurities of pollutants in the atmosphere, a special place is occupied by devices based on photo-acoustic spectroscopy [1–3]. They have high sensitivity and allow monitoring air in real time. Sulphur hexafluoride has a broad absorption band centered at 947.6 cm⁻¹ [4], which coincides with the band of CO₂ laser radiation at 10.6 μm [5]. Figure 1 shows the SF₆ absorption spectrum in the range of 900–1000 cm⁻¹ [6].

The aim of this work is to study the parameters of a high-sensitivity laser photo-acoustic SF₆ gas analyzer based on a CO₂ laser and resonant photo-acoustic detector.

2. ANALYSIS OF THE OPTICAL SCHEMES OF THE GAS ANALYZER

The possibility of constructing a highly sensitive photo-acoustic SF₆ gas analyzer based on a CO₂ laser was shown in [7]. Let us consider some of the optical circuits of the sulfur hexafluoride analyzer, which are shown in Fig. 2. The structure of these schemes includes a waveguide CO₂ laser, a resonant differential

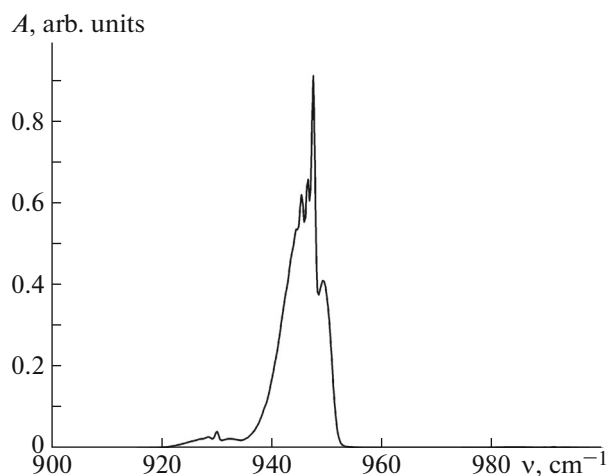


Fig. 1. The absorption spectrum of SF₆ in the range of 900–1000 cm⁻¹.

¹ The article was translated by the authors.

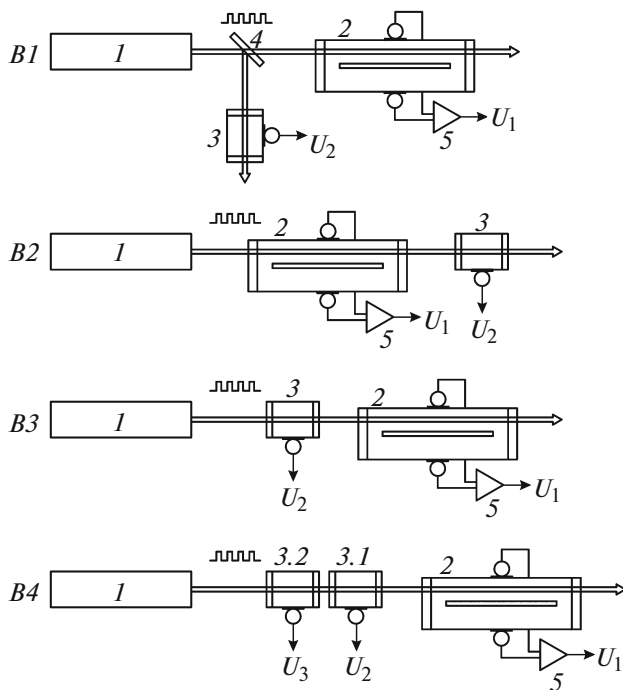


Fig. 2. The optical circuits of the laser photo-acoustic analyzer: 1, CO₂ laser; 2, resonant photo-acoustic detector; 3 (3.1, 3.2), sealed gas-filled cell; 4, beam splitter; 5, differential amplifier.

photo-acoustic detector (PAD) and a sealed gas-filled cell. The photo-acoustic detector and cell are filled with gas mixtures with an admixture of SF₆. The CO₂ laser operates in a free-running mode with a pulse repetition frequency that coincides with the PAD resonance frequency f_0 . The laser radiation wavelength is randomly tuned near 10.6 μm , but it falls within the absorption band of SF₆. The acoustic oscillations are formed in the PAD and cell due to the absorption of pulses of CO₂ laser radiation by SF₆ molecules that are recorded by microphones.

The resonant differential PAD has two parallel acoustic resonators [2, 8], where the acoustic oscillations have opposite phases at the resonance frequency f_0 . The electrical signals from the PAD microphones are fed to a differential amplifier, where the useful antiphase signals are doubled and parasitic-phase ones are effectively suppressed (for example, air pumping noise). The normalization of the resonant PAD signals is carried out on the signals from the microphone of the sealed gas-filled cell. The magnitude of these signals is proportional to the laser power absorbed in the cell. The registration and processing of electrical signals from the microphones of the PAD and cell are carried out at a frequency f_0 .

The operating principle of the considered optical circuits using a sealed gas-filled cell is that at the random tuning of the wavelength λ of the CO₂ laser radi-

ation the absorption cross section $\sigma(\lambda)$ of the SF₆ that fills the PAD and the cell will be changed simultaneously. Therefore, with the normalization of the resonant PAD signals on the signals of a gas-filled cell the full or partial compensation of the influence of tuning the wavelength λ on the result of SF₆ concentration measure is possible.

2.1. The B1 Optical Scheme

Consider the B1 optical circuit (see Fig. 2). The beam of CO₂ laser radiation is split by the partial reflector into two parts, one of which passes through a gas-filled cell and a second one passes through a resonant PAD. The reflection coefficient of the beam splitter is R ; the transmittance of the PAD and cell windows is T . Let us denote the SF₆ concentration into the resonant PAD as n_1 and that into a sealed gas-filled cell as n_2 . Then, the optical thickness of the PAD will be equal to $\tau_1 = n_1\sigma(\lambda)l_1$, where l_1 is the PAD length. Similarly, the optical thickness of the gas-filled cell is equal to $\tau_2 = n_2\sigma(\lambda)l_2$, where l_2 is the cell length. The ratio of the signals of the PAD (U_1), taken from the differential amplifier and the gas-filled cell (U_2) in the weak absorption ($\tau_1, \tau_2 < 1$) can be written as

$$\frac{U_1}{U_2} = \frac{(1-R)}{R} \frac{S_1(f_0)}{S_2(f_0)} \left[\frac{n_1\sigma(\lambda)l_1}{n_2\sigma(\lambda)l_2} \right], \quad (1)$$

where $S_1(f_0)$ and $S_2(f_0)$ are the sensitivities of the resonant PAD and gas-filled cell, respectively, on the PAD resonance frequency f_0 .

From expression (1) we can determine the concentration n_1 :

$$n_1 = C_{B1}(f_0) \frac{U_1}{U_2}, \quad (2)$$

where $C_{B1}(f_0) = \left[\frac{S_2(f_0)}{S_1(f_0)} \frac{R}{(1-R)} \frac{n_2 l_2}{l_1} \right]$ is a calibration factor, which does not contain terms that depend on the laser wavelength λ . In this case, the effect of the laser wavelength tuning can be fully compensated.

2.2. Optical Scheme B2

Consider the B2 optical circuit (see Fig. 2), in which the resonant PAD and a gas-filled cell are arranged coaxially. The beam of the CO₂ laser radiation passes through the PAD and then through the cell. In this case, in the weak absorption ($\tau_1, \tau_2 < 1$) the ratio of the U_1/U_2 signals can be written as

$$\frac{U_1}{U_2} = \frac{1}{T^2} \frac{S_1(f)}{S_2(f)} \left[\frac{n_1\sigma(\lambda)l_1}{n_2\sigma(\lambda)l_2} \right] e^{\tau_1}, \quad (3)$$

where we determine the value of the concentration n_1 :

$$n_1 = C_{B2}(f) \frac{U_1}{U_2} (1 + \tau_1), \quad (4)$$

where $C_{B2}(f) = \left[\frac{S_2(f)}{S_1(f)} \frac{T^2 n_2 l_2}{l_1} \right]$ is a calibration factor, which does not contain terms that depend on the laser wavelength λ .

Expression (4) contains a factor $(1 + \tau_1)$ that includes the optical thickness τ_1 ; therefore, it depends on the SF₆ absorption cross section $\sigma(\lambda)$ and measurable concentration of SF₆. The concentration n_1 in the PAD can vary within a wide range. At low values of n_1 , when the PAD optical thickness $\tau_1 < 0.01$, the relative measurement error determined by the factor $(1 + \tau_1)$ in the expression (4) will also be small ($< 1\%$). However, at high values of n_1 the PAD optical thickness τ_1 can exceed 0.1, which may lead to an increase in the relative measurement error caused by the influence of wavelength tuning to 10% or more.

2.3. Optical Scheme B3

Consider the *B3* optical circuit (see Fig. 2). A beam of CO₂ laser radiation passes through the gas-filled cell and then through the resonant PAD. In this case, in the weak absorption ($\tau_1, \tau_2 < 1$) the ratio of the U_1/U_2 signals can be written as

$$\frac{U_1}{U_2} = T^2 \frac{S_1(f)}{S_2(f)} \left[\frac{n_1 \sigma(\lambda) l_1}{n_2 \sigma(\lambda) l_2} \right] e^{-\tau_2}, \quad (5)$$

where we determine the value of the concentration n_1 :

$$n_1 = C_{B3}(f) \frac{U_1}{U_2} (1 + \tau_2), \quad (6)$$

where $C_{B3}(f) = \left[\frac{S_2(f)}{S_1(f)} \frac{1}{T^2} \frac{n_2 l_2}{l_1} \right]$ is a calibration factor, which does not contain terms that depend on the laser wavelength λ .

Expression (6) includes a factor $(1 + \tau_2)$ that contains the optical thickness τ_2 ; therefore, it depends on the SF₆ absorption cross section $\sigma(\lambda)$. The optimal choice of the design parameters of a sealed gas-filled cell (length l_2 and concentration n_2) can ensure that the optical thickness τ_2 of the cell will be approximately 0.02–0.03. The relative error of measurement of the concentration n_1 that is associated with the random tuning of the CO₂ laser radiation wavelength and is determined by the factor $(1 + \tau_2)$ in expression (6) will not exceed 2–3%, which is an acceptable level for the use of this optical scheme in a laser photo-acoustic SF₆ gas analyzer.

2.4. Optical Scheme B4

Consider the *B4* optical circuit (see Fig. 2) that contains a resonant PAD and two sealed gas-filled cells (3.1, 3.2) arranged coaxially to the PAD. In this case, the 3.2 cell is an addition compared with the *B3* scheme that was previously considered. The laser beam passes sequentially through both cells and then through the PAD. The other conditions are the same as before. In weak absorption ($\tau_1, \tau_2, \tau_3 < 1$) the $(U_1/U_2)(U_3/U_2)$ signal ratio can be written as

$$\left(\frac{U_1}{U_2} \right) \left(\frac{U_3}{U_2} \right) = \frac{S_1(f)}{S_2(f)} \frac{S_3(f)}{S_2(f)} \left[\frac{n_1 l_1}{n_2 l_2} \right] \frac{\tau_3}{\tau_2} e^{(\tau_3 - \tau_2)}, \quad (7)$$

where $\tau_3 = n_3 \sigma(\lambda) l_3$ is the optical thickness of the additional gas-filled cell 3.2; $n_3, l_3, S_3(f)$ are the concentration of the absorbing gas, the length, and the sensitivity of the additional gas-filled cells 3.2, respectively.

From expression (7) we determine the value of the concentration n_1 :

$$n_1 = C_{B4}(f) \frac{U_1 U_3}{U_2^2} \left[\frac{\tau_2}{\tau_3} e^{(\tau_2 - \tau_3)} \right], \quad (8)$$

where $C_{B4}(f) = \left[\frac{S_2(f) S_2(f) n_2 l_2}{S_1(f) S_3(f) l_1} \right]$ is a calibration factor that is independent of the wavelength of the laser radiation λ .

Note the last factor in the square brackets in expression (8). Provided $\tau_2 = \tau_3$ this factor is equal to 1. In this case, expression (8) can be rewritten as

$$n_1 = C_{B4}(f) \frac{U_1 U_3}{U_2^2}. \quad (9)$$

Thus, if two identical sealed gas-filled cells that have equal optical thickness are used in the optical circuit *B4* of a gas analyzer, the measured concentration n_1 in the PAD will not depend on the wavelength of laser radiation within the absorption band of SF₆. In this case, the influence of the wavelength instability can be fully compensated.

3. EXPERIMENTAL SCHEME

The experiments were carried out on a device based on the *B1, B2, B3* optical circuits described above (see Fig. 2). The experimental device includes a waveguide CO₂ laser, a resonant differential PAD, and a sealed gas-filled cell. A N₂ + 40 ppm SF₆ gas mixture was used in experiments, which was prepared at a gas-vacuum post with an accuracy of $\pm 5\%$ and stored in a standard high-pressure cylinder.

The waveguide CO₂ laser has a sealed cylindrical stainless steel housing with dimensions of $\text{Ø}60 \times 205$ mm. The active medium of the laser was a glow capacitive high-frequency discharge (144 MHz) in a gas mixture CO₂ : N₂ : He : Xe = 1 : 1 : 5 : 0.5 (the pressure is 120 Torr), which was excited in a square hollow wave-

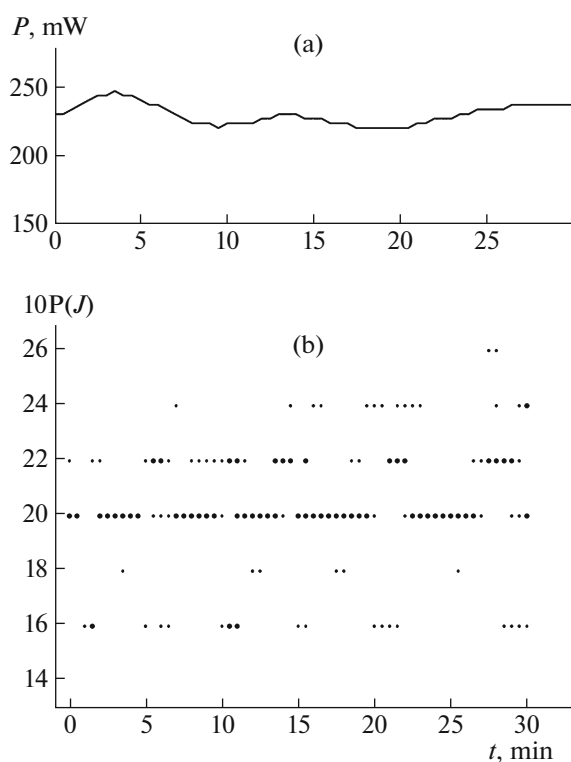


Fig. 3. Experimental dependences of the average power of waveguide CO₂ laser radiation (a) and tuning on emission lines (b) in 10P(J) band to time (J is the rotational number). Laser operation mode: pulse repetition frequency is 100 Hz; pulse duration is 100 μ s.

guide with dimensions of $1.8 \times 1.8 \times 150$ mm. A laser optical cavity with a length of $L = 155$ mm was formed by two flat mirrors. The transmittance of the output coupler was $T_1 = 8\%$ at a wavelength of $10.6 \mu\text{m}$; the rear reflector was gold plated. The intermode cavity interval $c/(2L)$ was ~ 1 GHz, while the width of the gain contour of the laser active medium did not exceed 600 MHz.

The differential resonant PAD [8] has two parallel cylindrical acoustic resonators with a size of $\text{O}9 \times 90$ mm. ZnSe windows with an AR coating at a wavelength of $10.6 \mu\text{m}$ are installed at the ends of the detector. The PAD lower resonance frequency f_0 at room temperature is 1757 Hz (air) or 1784 Hz (nitrogen). Such detectors were used previously in [9, 10].

The sealed gas-filled cell is a cylindrical glass cell with a size of $\text{O}12 \times 12$ mm, for which ZnSe windows with an AR coating at a wavelength of $10.6 \mu\text{m}$ are glued to the ends. A microphone is placed on the side wall of the cell connected to the inner volume. The cell was filled with a gas mixture of $\text{N}_2 + 40$ ppm SF_6 up to atmospheric pressure and then sealed. Under these conditions the optical thickness of the gas-filled cell τ_2 does not exceed 0.03 based on the data of the SF_6 absorption coefficient [4].

In the experiments, a waveguide CO₂ laser operated in the free-running mode with different pulse repeti-

tion frequencies. In this case, the laser wavelength was tuned randomly around the value $\lambda = 10.6 \mu\text{m}$ on various emission lines. Figure 3 shows the experimental record for 30 min average output power (Fig. 3a) and the laser emission lines (Fig. 3b). The laser operated with a pulse repetition rate of 100 Hz with a pulse duration of 100 μs . The power of the laser radiation was determined using an IMO-2N meter. During the observation period the average power of the laser varied in the range of 220–250 mW (see Fig. 3a); the peak power of radiation pulses reached 25 W.

A manual scan of the spectral bandwidth of an upgraded IKS-10 monochromator was carried out when the spectrum of the CO₂ laser radiation was recorded (Fig. 3b). In the experiment the actual emission line of the CO₂ laser with a different power was fixed during 30 min at intervals of 30 s. Figure 3b indicates the dominant laser emission lines at the moment of scanning via large dots and emission low-power satellite lines via small dots. During the observation time the different emission lines in the spectrum of CO₂ laser radiation were detected in the 10P(16)–10P(26) range. For most of the observation time the laser operated on the 10P(20) line. One to two additional satellite lines were almost always present in the radiation. During observation the spectral range of the wavelength tuning of the CO₂ laser radiation did not go beyond the broad SF_6 absorption band [4].

4. EXPERIMENTAL RESULTS

4.1. Determination of Operating Conditions

At the beginning of the series of experiments using the B3 optical circuit the frequency responses of the resonant PAD (U_1) and gas-filled cells (U_2), the ratio of their signals (U_1/U_2), and the phase ratio were investigated around the PAD resonance frequency f_0 . The results are shown in Fig. 4. In this experiment a CO₂ laser with a diffraction grating was used to eliminate the influence of wavelength tuning [11], which radiated on the fixed line 10P(20). The pulse-repetition frequency of CO₂ laser radiation was continuously tunable in the range of 1600–2000 Hz and the pulse duration was 50 μs . The resonant PAD was filled with a $\text{N}_2 + 40$ ppm SF_6 gas mixture. At the same time, taking the data on the absorption coefficient of SF_6 [4] PAD into account, the optical thickness τ_1 did not exceed 0.25.

Figure 4a shows a fragment of the resonant PAD response (U_1) near the resonance frequency $f_0 \approx 1790$ Hz. Figure 4b gives a fragment of the response of the sealed gas-filled cell (U_2), which has the form of a straight line with a slight slope. During scanning, the repetition rate of the laser pulses gradually increased, but the pulse duration remained constant; thus, the average power of the CO₂ laser radiation increased with the increase in the pulse-repetition frequency. Thus, it can

be considered that the response of a gas-filled cell proportional to the average laser power is practically linear in the 1600–2000 Hz range and independent of frequency.

Figure 4c shows an experimental record of the (U_1/U_2) ratio of the signals of a resonant PAD and a gas-filled cell in the 1600–2000 Hz frequency range. The ratio of the signals U_1/U_2 practically repeats the PAD resonance at $f_0 \approx 1790$ Hz [8]. Note that measurement of the SF₆ concentration n_1 should be carried out precisely at the PAD resonance frequency f_0 , which required determining it directly during concentration measurements.

Figure 4d shows the variation of the phase difference $\Delta\varphi(f)$ between the signals of the resonant PAD (U_1) and gas-filled cell (U_2) in the frequency range of 1600–2000 Hz. Around the PAD resonance frequency the phase difference changes by 180°, while at the PAD resonant frequency (1790 Hz) $\Delta\varphi = 90^\circ$.

In [8] a method for measuring the PAD resonance frequency in real time over a wide variation range of temperature and gas mixtures composition was proposed. The algorithm is based on measuring of the natural frequencies of the resonant PAD, which are excited by an auxiliary acoustic emitter, a built-in PAD. The measurement procedure takes 0.1 s or less. The relative error in the measurement of the PAD resonance frequency was $\sim 6 \times 10^{-5}$.

4.2. Investigation of Optical Circuits

Experimental studies of the $B1$, $B2$, $B3$ optical circuits were carried out when the resonant PAD was filled with an N₂ + 40 ppm SF₆ gas mixture. The PAD resonance frequency was $f_0 = 1790$ Hz. A flat ZnSe plate was used in the $B1$ circuit for splitting the radiation beam of the CO₂ laser (see Fig. 2), set at an angle close to the normal incidence. This reflectivity R of the splitting plate was ~ 0.3 . The calibration procedure of the analyzer was carried out for each circuit ($B1$, $B2$, $B3$) and the calibration factors $C_{B1}(f_0)$, $C_{B2}(f_0)$, $C_{B3}(f_0)$ included in expressions (2), (4), (6) were experimentally measured.

Figure 5a shows the experimental records of signals of a resonant PAD (U_1), a sealed gas-filled cell (U_2) and the measured SF₆ concentrations (n_1) using the $B3$ optical circuit. Similar records with a duration of 20 min were also made for the $B1$ and $B2$ circuits. Graphs for the concentration n_1 are obtained from the U_1/U_2 ratio of the signals, taking the pre-calibration of the gas analyzer into account. Due to the spontaneous tuning of the wavelength λ of the CO₂ laser radiation near 10.6 μm and the associated changes in the SF₆ absorption cross section $\sigma(\lambda)$, the signals of the resonant PAD (U_1) and gas-filled cell (U_2) experienced a significant (up to $\sim 50\%$), but almost simultaneous

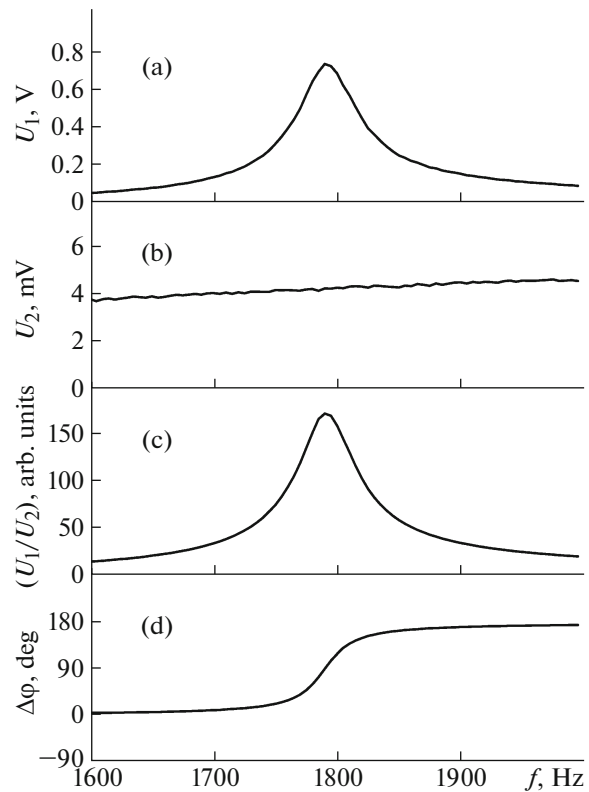


Fig. 4. The experimental dependences: (a), the responses of the resonant PAD (U_1); (b), a sealed gas-filled cell (U_2); (c), signal ratio U_1/U_2 ; (d), phase difference $\Delta\varphi$ at the repetition frequency of CO₂ laser pulses in the range of 1600–2000 Hz (optical circuit $B3$).

variation. However, the graphs of the measured concentration n_1 showed a much smaller level of variation.

For all the circuits ($B1$, $B2$, $B3$) when the resonant PAD was filled with a N₂ + 40 ppm SF₆ gas mixture the value of the measured concentration n_1 fluctuated around 40 ppm: in the range of ~ 36 –46 ppm (± 13 –15%) for the $B1$ scheme; ~ 38.6 –41.2 ppm ($\pm (3$ –4)%) for the $B2$ scheme; and ~ 38.3 –41.4 ppm ($\pm (3$ –4)%) for the $B3$ scheme. Series of repeated experiments showed similar results. Thus, in the experiment the $B1$ optical circuit with a beam splitter showed the worst result for the compensation of the influence of the spontaneous tuning of the CO₂ laser wavelength, although expression (2) predicted the opposite result.

Next, the experiment using the $B3$ optical circuit during pumping of an air flow with a small admixture of SF₆ (less than 100 ppb) through the resonant PAD was carried out. Such conditions are typical for the actual operation of the SF₆ gas analyzer to detect leaks. In the experiment, the standard control SF₆ leakage was used, which at the time of calibration (February 2010) had an intensity $I = 1.02 \times 10^{-7}$ m³ Pa/s. With time, up to the moment of this experiment (September 2015), the intensity of the control leakage continu-

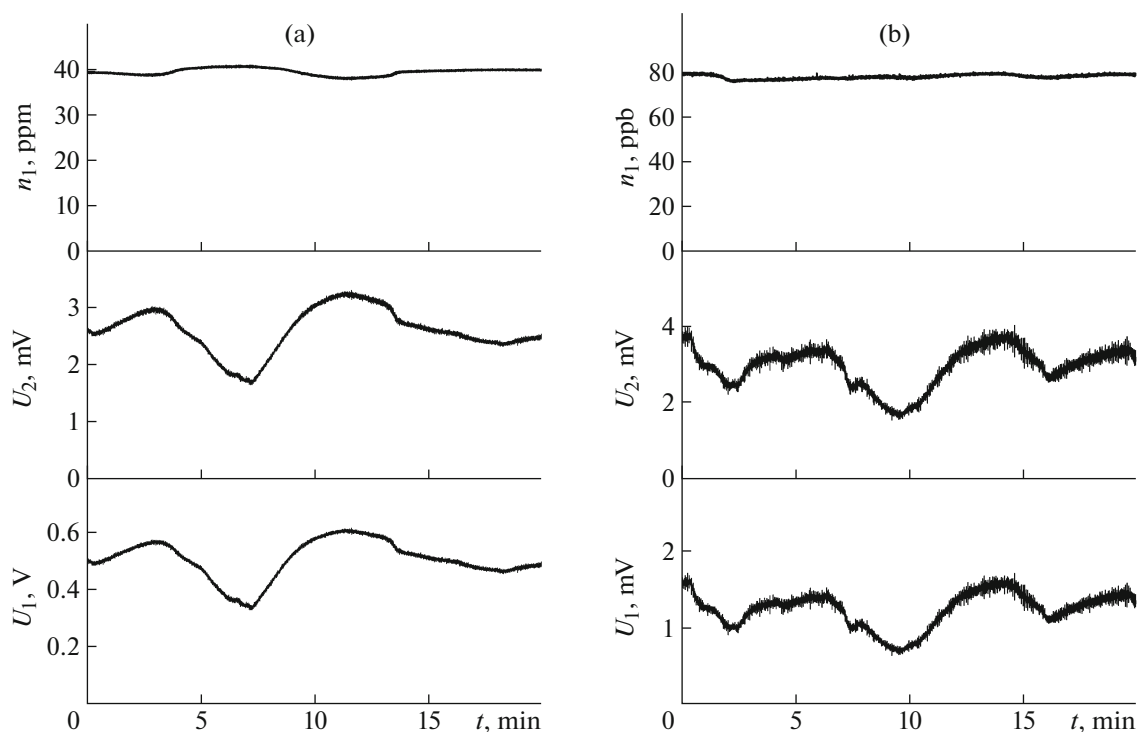


Fig. 5. Experimental records of the signals of the resonant PAD (U_1), a sealed gas-filled cell (U_2), the concentration of SF_6 (n_1) for the *B3* optical circuit when filling the PAD $\text{N}_2 + 40$ ppm SF_6 gas mixture (a) or by pumping air through the PAD at a rate of 0.6 L/min with ~ 80 ppb SF_6 impurity (b).

ously declined by approximately 20%, which was fixed by periodic measurements.

An air pump was used for air flow through the PAD. The flow rate of 0.6 L/min was controlled by a gas-flow meter (RMA-0.063 GUZ). Air was taken from the outlet of the control SF_6 leakage. As a result, the flow of SF_6 from the control leakage was added to the flow of air sucked by the pump and the air flow with an admixture of approximately 80 ppb SF_6 was pumped through the PAD. The PAD resonance frequency was approximately 1760 Hz. Figure 5b shows the experimental records of the signals of the resonant PAD (U_1), a sealed gas-filled cell (U_2), and the measured SF_6 concentration n_1 in the air stream. The graph of the concentration n_1 over 20 min experienced variations around values of ~ 78 ppb in the range of 75–80 ppb ($\pm(3\text{--}4)\%$).

Figure 6a shows the experimental records of SF_6 concentration measurements in different conditions when using the *B3* optical circuit. The schedule consists of four fragments of 1 min each: 1, the resonant PAD was filled with a $\text{N}_2 + 40$ ppm SF_6 gas mixture; 2, for air flow (0.6 L/min) through a resonant PAD with an admixture of approximately 80 ppb SF_6 ; 3, the record of the background when pumping pure air through the resonant PAD; and 4, the noise path in the mode of subtracting the average background value.

According to Fig. 6a, during the pumping of pure air through the resonant PAD the background value of the measured SF_6 concentration was $\sim 0.8\text{--}1$ ppb. The procedure of averaging and memorizing the background (for ~ 10 s) and subtracting it under the same conditions revealed that the average noise level in the “background subtraction” is approximately 0.1 ppb SF_6 . The experimental results of the SF_6 detection limit the sensitivity in the air stream obtained in this paper at an order of magnitude comparable with the results of [12].

Figure 6b shows the results of experimental measurement of the phase difference ($\Delta\phi$) of the signals of the resonant PAD (U_1) and a sealed gas-filled cell (U_2) measured at different levels of SF_6 concentration. The schedule consists of three fragments, 2 min each corresponding to the same conditions as in Fig. 6a. When the resonant PAD was filled with a gas mixture consisting of an admixture of SF_6 (40 ppm or ~ 78 ppb) the phase difference was $\Delta\phi \approx 90^\circ$. In both cases, the absorption of CO_2 laser radiation pulses by SF_6 molecules occurred in the resonant PAD. However, when pumping clean air through the resonant PAD the absorption in the PAD did not occur and the phase difference was $\sim 180^\circ$. Thus, the phase of the desired signal of the resonant PAD in the presence of radiation absorption by SF_6 molecules differs from the phase of the background (noise) signal corresponding to the

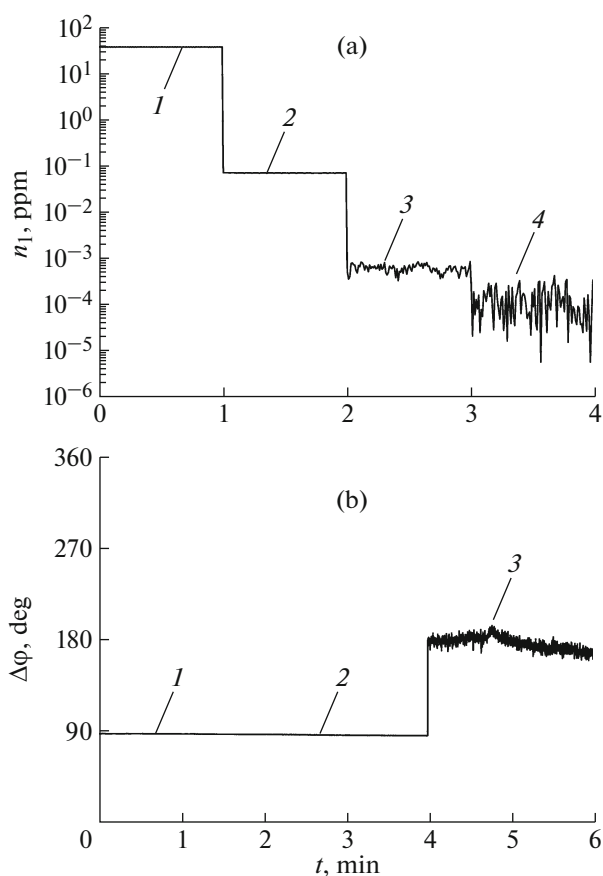


Fig. 6. Experimental records of various SF_6 concentrations measurements (a) and phase difference of U_1 and U_2 signals (b) using the optical circuit B3: 1, $\text{N}_2 + 40$ ppm SF_6 gas mixture; 2, air pumping through the PAD (0.6 L/min) with an admixture of ~ 80 ppb SF_6 ; 3, pumping clean air through the PAD (background); 4, pumping clean air through the PAD in the “background subtraction” mode.

pumping of clean air around $\pi/2$. This makes it possible in practice to effectively suppress background noise using the synchronous signal-detection method. In this phase the measuring system must be adjusted to the maximum of the absorption signal in the resonant PAD.

5. CONCLUSIONS

In this paper we considered a number of optical circuits for the construction of a laser photo-acoustic SF_6 gas analyzer based on a CO_2 laser, a resonant differential photo-acoustic detector, and a sealed gas-filled cell. It is proposed to carry out the normalization of the signals of a resonant PAD on the signals of a gas-filled cell that are proportional to the radiation power absorbed by SF_6 molecules. In this case, it is possible to compensate for the influence of wavelength tuning of the CO_2 laser emission near $10.6 \mu\text{m}$ based on the measurement results of the SF_6 concentration.

Experimental studies of laser photo-acoustic gas analyzer were carried out at different concentrations of

SF_6 , including in the air flow. The limit sensitivity of the developed laser photo-acoustic gas analyzer is ~ 1 ppb SF_6 . It was experimentally shown that the relative error of the measurements of the SF_6 concentration due to the tuning of the emission wavelength of the CO_2 laser did not exceed $\pm 5\%$ over the entire range from ~ 80 ppb to 40 ppm.

ACKNOWLEDGMENTS

The authors thank Dr. Karapuzikov A.I. (Institute of Laser Physics SB RAS, Novosibirsk, Russia), Prof. Ponomarev Yu.N., Dr. Kapitanov V.A. (both from the Institute of Atmospheric Optics, SB RAS, Tomsk, Russia) for help with the work, useful discussions and comments. This work was supported by Special Technology, Ltd. (Novosibirsk, Russia).

REFERENCES

1. Harren, F.J.M., Bijnen, F.G.C., Reuss, J., Voese-nek, L.A.C.J., and Blom, C.W.P.M., *Appl. Phys. B*, 1990, vol. 50, no. 2, p. 137. doi 10.1007/BF00331909
2. Miklos, A., Hess, P., and Bozoki, Z., *Rev. Sci. Instrum.* 2001, vol. 72, no. 4, p. 1937. doi 10.1063/1.1353198
3. Ponomarev, Yu.N., Ageev, B.G., Zigris, M.V., Kapitanov, V.A., Kurtua, D., and Nikiforova, P.Yu., *Lazernaya optikoakusticheskaya spektroskopiya mezhmolekulyarnykh vzaimodeystvii v gazakh* (Laser Opticoacoustic Spectroscopy of Intermolecular Interactions in Gases), Sinitsa, L.N., Ed., Tomsk: MGP RASKO, 2000.
4. Cox, D.M., and Gnauck, A., *J. Mol. Spectrosc.*, 1980, vol. 81, no. 1, p. 207. doi 10.1016/0022-2852(80)90338-0
5. Witteman, W.J., *The CO_2 -Laser*, Berlin: Springer-Verlag, 1990; Moscow: Mir, 1990.
6. NIST Standard Reference Database: <http://webbook.nist.gov/chemistry/>
7. Sherstov, I.V., Kapitanov, V.A., Ageev, B.G., Karapuzikov, A.I., and Ponomarev, Yu.N., *Atmosph. Ocean. Optics*, 2004, vol. 17, nos. 2–3, p. 102.
8. Sherstov, I.V., Vasiliev, V.A., Goncharenko, A.M., Zenov, K.G., Pustovalova, R.V., and Karapuzikov, A.I., *Instrum. Exp. Tech.*, 2016, vol. 59, no. 5, p. 133. doi 10.7868/S0032816216050098
9. Lee, Ch.-M., Bychkov, K.V., Kapitanov, V.A., Karapuzikov, A.I., Ponomarev, Yu.N., Sherstov, I.V., and Vasiliev, V.A., *Opt. Eng.*, 2007, vol. 46, no. 6, p. 064302. doi 10.1117/1.2748042
10. Karapuzikov, A.I., Sherstov, I.V., Ageev, B.G., Kapitanov, V.A., and Ponomarev, Yu.N., *Atmosph. Ocean. Optics*, 2007, vol. 20, no. 5, p. 418.
11. Sherstov, I.V., Bychkov, K.V., Vasiliev, V.A., Karapuzikov, A.I., Spitsyn, V.V., and Chernikov, S.B., *Atmosph. Ocean. Optics*, 2005, vol. 18, no. 3, p. 248.
12. Sampaolo, A., Patimisco, P., Giglio, M., Chieco, L., Scamarcio, G., Tittel, F.K., and Spagnolo, V., *Optics Exp.*, 2016, vol. 24, no. 14, p. 15872. doi 10.1364/OE.24.015872